JACS
JOURNAL OF THE AMERICAN CHEMICAL SOCIETY
pubs.acs.org/JACS
Article

One-Component Multifunctional Sequence-Defined Ionizable Amphiphilic Janus Dendrimer Delivery Systems for mRNA

Dapeng Zhang,[♦] Elena N. Atochina-Vasserman,[♦] Devendra S. Maurya, Ning Huang, Qi Xiao, Nathan Ona, Matthew Liu, Hamna Shahnawaz, Houping Ni, Kyunghee Kim, Margaret M. Billingsley, Darrin J. Pochan, Michael J. Mitchell, Drew Weissman,* and Virgil Percec*

Cite This: https://doi.org/10.1021/jacs.1c05813

ABSTRACT: Efficient viral or nonviral delivery of nucleic acids is the key step of genetic nanomedicine. Both viral and synthetic vectors have been successfully employed for genetic delivery with recent examples being DNA, adenoviral, and mRNA-based Covid-19 vaccines. Viral vectors can be target specific and very efficient but can also mediate severe immune response, cell toxicity, and mutations. Four-component lipid nanoparticles (LNPs) containing ionizable lipids, phospholipids, cholesterol for mechanical properties, and PEG-conjugated lipid for stability represent the current leading nonviral vectors for mRNA. However, the segregation of the neutral ionizable lipid as droplets in the core of the LNP, the "PEG dilemma", and the stability at only very low temperatures limit their efficiency. Here, we report the development of a one-component multifunctional ionizable amphiphilic Janus dendrimer (IAJD) delivery system for mRNA that exhibits high activity at a low concentration of ionizable amines organized in a sequence-defined arrangement. Six libraries containing 54 sequence-defined IAJDs were synthesized by an accelerated modular-orthogonal methodology and coassembled with mRNA into dendrimersome nanoparticles (DNPs) by a simple injection method rather than by the complex microfluidic technology often used for LNPs. Forty four (81%) showed activity *in vitro* and 31 (57%) *in vivo*. Some, exhibiting organ specificity, are stable at 5 °C and demonstrated higher transfection efficiency than positive control experiments *in vitro* and *in vivo*. Aside from practical applications, this proof of concept will help elucidate the mechanisms of packaging and release of mRNA from DNPs as a function of ionizable amine concentration, their sequence, and constitutional isomerism of IAJDs.

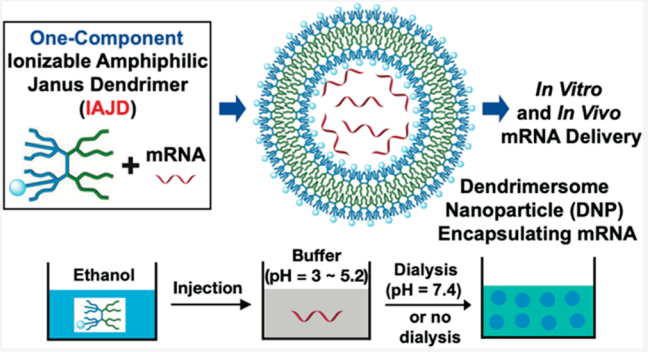

INTRODUCTION

The delivery of exogenously produced nucleic acids into cells and/or their nucleus to modify protein expression by viral and nonviral vectors represents one of the most fundamental concepts of nanomedicine.[1] Both viral and nonviral delivery systems exhibit advantages and disadvantages. Viral vectors have high transfection efficiency (95%)[1a] and higher specificity for cell targeting including for unnatural cells.[1g] Some drawbacks of viral gene delivery include immunogenicity,[2a] cytotoxicity,[2b] difficulty of assembly,[2c] inflammatory responses to repeated administration,[1h] and the potential for insertional mutagenesis.[1f] Nonviral delivery has higher biosafety and exhibits lower toxicity and immunogenicity, but it is less transfection efficient (1−2%)[1f] and the vectors are less stable than the viral ones.[1h] Covalent[3a−f] and supramolecular dendrimers[3g−i] complexed on their cationic periphery groups with the nucleic acid have been employed as nonviral vectors for cell transfection of DNA. Four-component lipid nanoparticles (LNPs)[1e,4] containing ionizable lipids,[4a,b] phospholipids, cholesterol for improved mechanical properties, and a PEG-conjugated lipid that provides stability represents the current leading nonviral vector for the delivery of mRNA. Shortcomings of LNP production and stability are exemplified by a T-tube of a microfluidic device required for their assembly[6] and the need for long-term storage at extremely low temperatures (−70 °C).[1k] Their design, synthesis, and assembly were inspired from that of stealth liposomes developed to deliver low molar mass drugs.[5] Since RNA is less stable than DNA due to enzymatic degradation, it must be protected by encapsulation before being released in the cell. At acidic pH (pH 3 to 5) LNPs can encapsulate large quantities of mRNA when the pK_a of the ionizable amine is less than 7.[1i,7] At physiological pH (7.4)[7] LNPs have a nearly neutral surface

Received: June 4, 2021

charge and a high positive charge at the endosomal pH. In endosomal membranes the electrostatic interaction between the cationically charged LNPs and the naturally occurring anionic lipids was suggested to be responsible for the release of the RNA.[7] One of the major limitations of the four-component vector is the unknown distribution of its four components in the LNP. The segregation of the neutral ionizable lipid as an oil phase in the core of the LNPs is considered to be responsible for their very low transfection efficiency (1−2%).[7] The second deficiency of the LNP originating from the PEG-conjugated lipid is known as the "PEG dilemma".[8] The PEG conjugated to LNP increases their circulation time in the blood after intravenous injection. However, the same PEG-LNP is known to decrease gene expression by up to 4 orders of magnitude by reducing intracellular trafficking of cellular uptake and endosomal escape.[8]

A charge-altering releasable transporter concept for the delivery of mRNA was recently elaborated by the Waymouth laboratory.[9] This new delivery protocol is unrelated to the viral and nonviral LNP-based methodologies discussed above. Artificial and synthetic vesicles, such as liposomes[10] and polymersomes,[11] have been elaborated for both drug delivery and also as mimics of natural cells. Our laboratory developed a new class of synthetic vesicles with excellent mechanical properties and stability including in serum, named dendrimersomes (DSs), which are assembled from amphiphilic Janus dendrimers (JDs).[12] Amphiphilic JDs with sugars conjugated on their hydrophilic region, denoted Janus glycodendrimers (JGDs), self-assemble into glycodendrimersomes (GDSs), which mimic the glycans of biological membranes and bind sugar-binding proteins.[12] Both JDs and JGDs self-assemble into monodisperse DSs and GDSs with unilamellar or multilamellar structures by simple injection rather than by the microfluidic technology, and their dimensions can be predicted.[12a−e,13a−c] Sequence-defined JGDs[13b−f] self-assemble by simple injection into GDSs. It has been demonstrated that a lower sugar density in a defined sequence elicits higher bioactivity to sugar-binding proteins.[13b−d,f] This concept informs a design principle for active soft and living matter with potential applications in cellular biology[12f−k,d] and gene delivery.[12i] The goal of this publication is to report the design of a one-component multifunctional sequence-defined ionizable amphiphilic Janus dendrimer (IAJD) delivery system that coassembles with mRNA by simple injection into dendrimersome nanoparticles (DNPs) using principles elaborated with JDs and JGDs.[12,13] Screening experiments with six libraries containing 54 IAJDs were performed both *in vitro* and *in vivo*. They demonstrated the proof of concept of DNPs, their potential applications, and utility as a model to elucidate fundamental aspects of the complex nonviral delivery systems and as future delivery systems for mRNA-based therapeutics.

RESULTS AND DISCUSSION

A Brief Comparison of the Four-Component LNPs with One-Component DNPs. One of the major advantages of the synthetic vectors used for the delivery of mRNA consists in their unlimited synthetic capabilities. The transformation of the four-component LNP into a one-component DNP represents a demonstration of this synthetic capability (Figure 1). Figure 1a illustrates the process involved in the assembly of one-component LNPs. The four-component composition containing various ratios of the ionizable lipid, phospholipid, PEG-lipid, and cholesterol is prepared as a solution in ethanol.

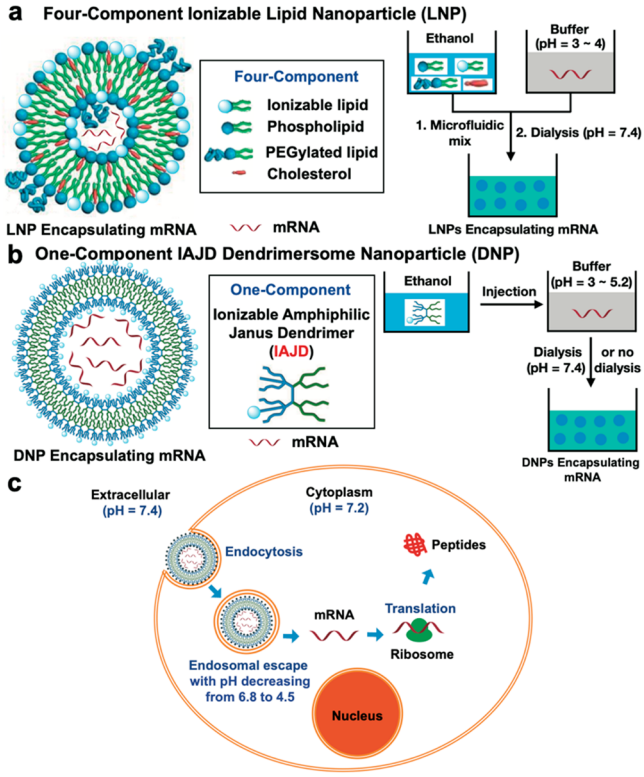

Figure 1. Schematic representation of (a) four-component LNPs for mRNA delivery; (b) one-component DNPs for mRNA delivery; (c) cell-entry and release process of the LNP or DNP.

This ethanol solution is mixed with a microfluidic device or T-tube with a pH 3 to 5 buffer solution and with an aqueous solution of mRNA. The mRNA used in the acidic buffer solution is produced and stored in neutral water. The resulting nanoparticles containing mRNA are analyzed by dynamic light scattering (DLS) to determine the diameter (D, nm) and the polydispersity index (PDI) of the LNPs, dialyzed to pH 7.4, analyzed by DLS again, and stored at −70 °C before the *in vitro* or *in vivo* experiments were performed.

Figure 1b illustrates the same process for the one-component DNPs. The IAJD containing an ionizable amine incorporated in a precise sequence is dissolved in ethanol. The ethanol solution is injected into an acidic buffer solution containing mRNA (pH 3 to 5.2). Depending on the original pH of the buffer, the resulting DNPs containing mRNA already have a pH between 4.5 and 7.3 and after DLS analysis can be used for *in vitro* and *in vivo* experiments before or after dialysis. Long-term storage of DNPs is at 5 °C. Figure 1c illustrates the schematic transition from the extracellular to the intracellular process for both LNPs and DNPs. Once injected, both the LNP and DNP approach the corresponding cells and get encapsulated via endocytosis. The extracellular pH is 7.4, and therefore, LNPs and DNPs enter the cell with an almost neutral surface. Subsequently, the endocytosis of LNPs or DNPs deposits them into endosomes, the pH of which decreases from 6.8 to 4.5 during their maturation into lysosomes due to ATP-dependent proton pumps on the endosomal membrane.[15] Therefore, both LNPs and DNPs get reprotonated, interact with the naturally occurring anionic lipids, and release the mRNA into the cytoplasm, which allows the ribosome to generate the new proteins.[4] When the ionizable amines from LNPs are segregated in their center,

https://doi.org/10.1021/jacs.1c05813
J. Am. Chem. Soc. XXXX, XXX, XXX−XXX

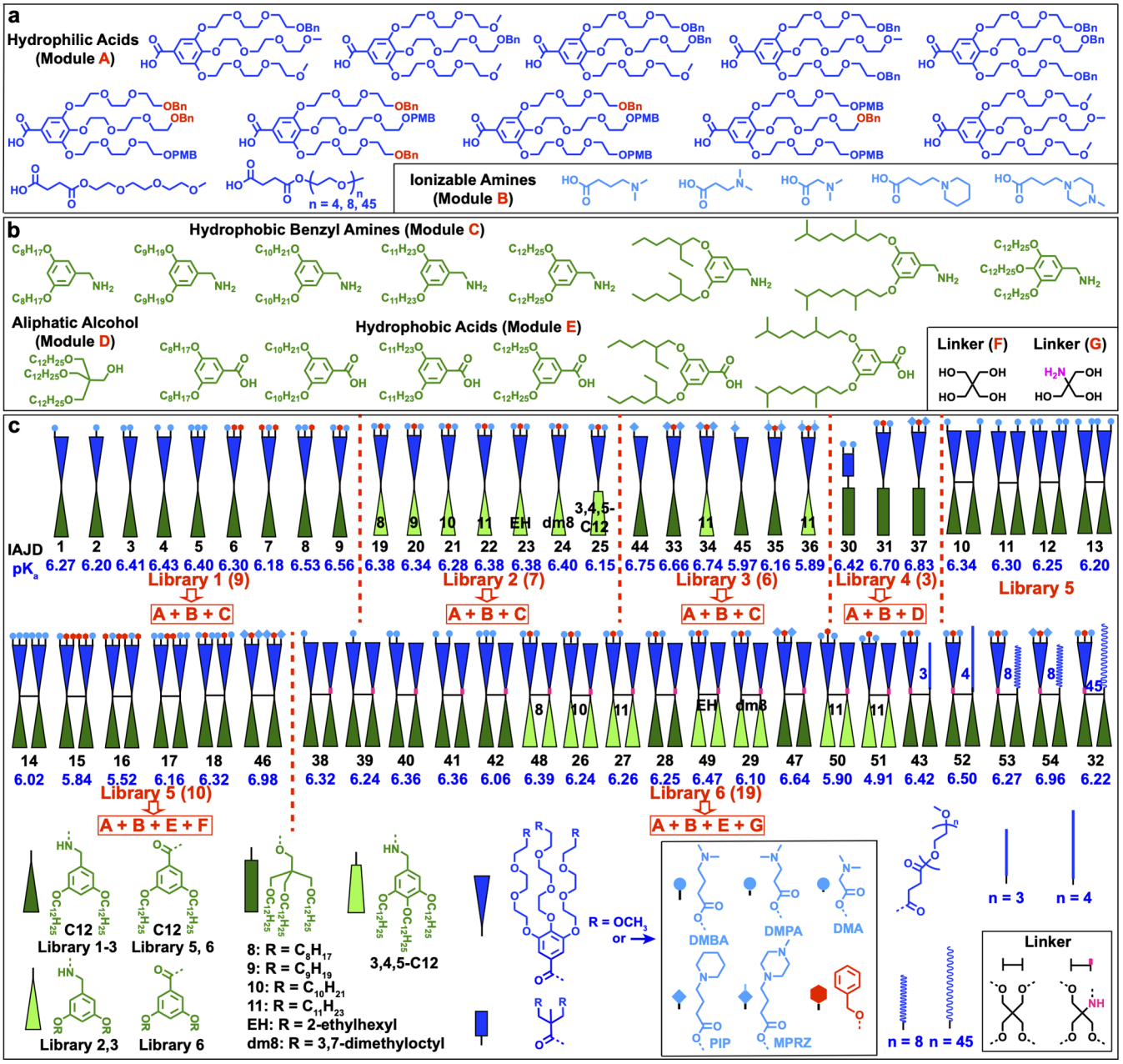

Figure 2. Schematic representation of the six libraries of 54 sequence-defined IAJDs (c). Structures of all their modules (a, b). The accelerated modular-orthogonal synthesis of IAJDs is outlined in (c).

reprotonation of their periphery cannot occur, and as a result, the release of mRNA in the cell has reduced efficiency (1−2%).[4]

Accelerated Modular-Orthogonal Synthesis of the Six Libraries of IAJDs. Modular-orthogonal methodologies for the synthesis of sequence-defined amphiphilic Janus glycodendrimers were elaborated by our laboratory.[12,13] Accelerated modular-orthogonal methodologies (Figure 2) for the synthesis of single−single (a single hydrophobic combined with a single hydrophilic dendron),[12d,e,j] twin−twin (two identical hydrophobic and two identical hydrophilic dendrons),[12a,a] and hybrid twin-mix (two identical hydrophobic and two different hydrophilic dendrons)[13b−f] rely on related but improved and accelerated synthetic principles originally developed and employed for the synthesis of sequence-defined JGDs.[12b,13b−f] Two different orthogonal protective groups, 4-methoxybenzyl ether and benzyl ether, were employed in the new methodology.[16] The six libraries synthesized are schematically shown in Figure 2c. Four of these libraries are based on single−single IAJDs. Nine IAJDs are available in library 1, seven in library 2, six in library 3, and three in library 4. Library 5 is based on the twin−twin IAJDs generated from IAJD1 to IAJD9 of library 1 and IAJD33 of library 3. Library 6 contains 19 hybrid twin-mix IAJDs selected from all libraries. The selection process was determined by the activity *in vivo* and *in vitro* of their single−single components, and the number associated with the corresponding IAJD illustrates the design process driven by DNP activity. The hydrophilic parts of these IAJDs contain sequence-defined compositions based on the dimethylaminobutanoate (DMBA), dimethylaminopropanoate (DMPA), dimethylaminoacetate (DMA), piperidinebutanoate (PIP), and methylpiperazinebu-

https://doi.org/10.1021/jacs.1c05813
J. Am. Chem. Soc. XXXX, XXX, XXX−XXX

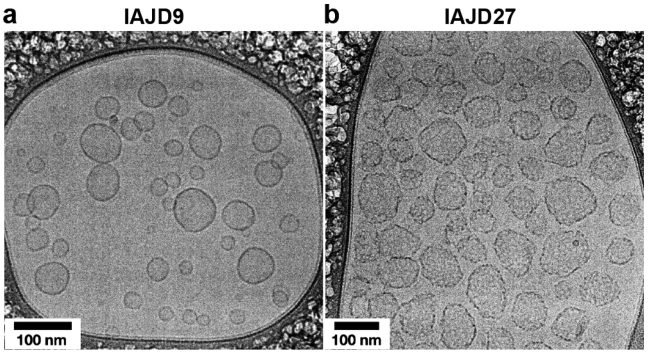

Figure 3. Cryo-TEM images of DNP vesicles self-assembled from IAJD9 (a) and from IAJD27 (b) in the absence of mRNA in TRIS buffer (4.0 mg/mL, pH = 7.4). Their dimensions determined by DLS (D = 92 nm, PDI = 0.238 for IAJD9 assemblies and D = 75 nm, PDI = 0.201 for IAJD27 assemblies) match very well the data from the cryo-TEM experiments. Vesicles of IAJD27 contain *n*-undecyl groups in their hydrophobic part and seem more fragile[12m] than the vesicles of IAJD9 containing *n*-dodecyl groups.

tanoate (MPRZ) ionizable amines (Figure 2a module A, module B, and the box from the bottom part of Figure 2c).

They were selected based on the pK_a of their corresponding ionizable lipids available in the literature.[4a,14] The symbols employed in the schematic representation of these sequence-defined IAJDs are shown in the square from the bottom part of Figure 2c. A benzyl ether group, marked in red, was employed to isolate the ionizable amines and construct different sequences in the hydrophilic part of the IAJDs. Aromatic groups such as benzyl ethers are known to interact as hydrogen-bond acceptors in molecular recognition with cations including ammonium groups both in biology and in synthetic supramolecular chemistry.[17] This cation−π interaction is weaker than the traditional H-bond (about 3 kcal/mol)[17a] and, therefore, can mediate a dynamic control of the pK_a of the ionizable amines. In the protonated state of the amine, the cation−π interaction can increase its pK_a[17] while in the nonprotonated state it may facilitate an interaction of the benzyl ether with the nucleic bases of the mRNA to enhance coassembly or segregate in the hydrophobic part of the DNPs to stabilize the assembly. To our knowledge, this cation−π interaction was not employed before in the design of nonviral delivery vectors for mRNA. The hydrophobic parts of the IAJDs contain both linear and branched alkyl groups of different length (Figure 2b, modules C, D, E, Figure 2c, Scheme S3). The hydrophilic acid components of these IAJDs are shown in Figure 2a (module A) and Figure S1, while their synthesis is described in Scheme S1. The structures of the hydrophobic benzyl amines are shown in Figure 2b (module C). Their synthesis is shown in Scheme S2. Combining all these modules in an orthogonal way, as illustrated in Figure 2c, provides, in an accelerated manner, the six libraries of IAJDs. The synthesis of the twin−twin part of the hydrophobic IAJDs is illustrated in Scheme S4. The synthesis of library 1 is shown in Scheme S5, of library 2 in Scheme S6, of library 3 in Scheme S7, of library 4 in Scheme S8, of library 5 in Scheme S9, and of library 6 in Schemes S10, S11, and S12. The detailed structures of all libraries of IAJDs together with their pK_a values and short

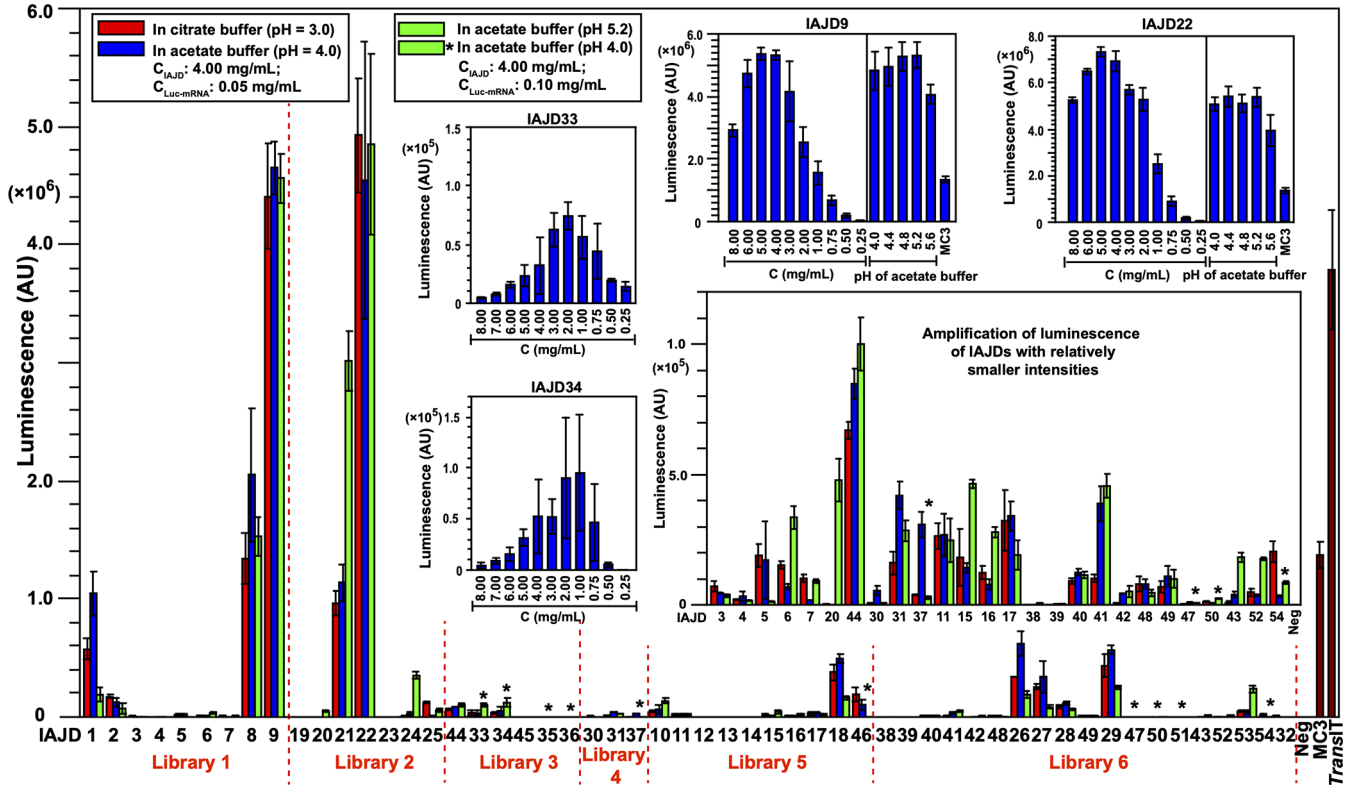

Figure 4. Luciferase expression in HEK293T cells with DNPs encapsulating luciferase-mRNA. Color codes for the self-assembly conditions of DNPs are in the top left corner. The two left-side insets show luminescence vs concentration dependences for IAJD33- and IAJD34-based DNPs. The top right-side insets show luminescence vs concentration and pH dependences for IAJD9- and IAJD22-based DNPs. Data have been calculated and represented as mean ± SD (standard deviation). Each experiment was performed at least three times.

https://doi.org/10.1021/jacs.1c05813
J. Am. Chem. Soc. XXXX, XXX, XXX−XXX

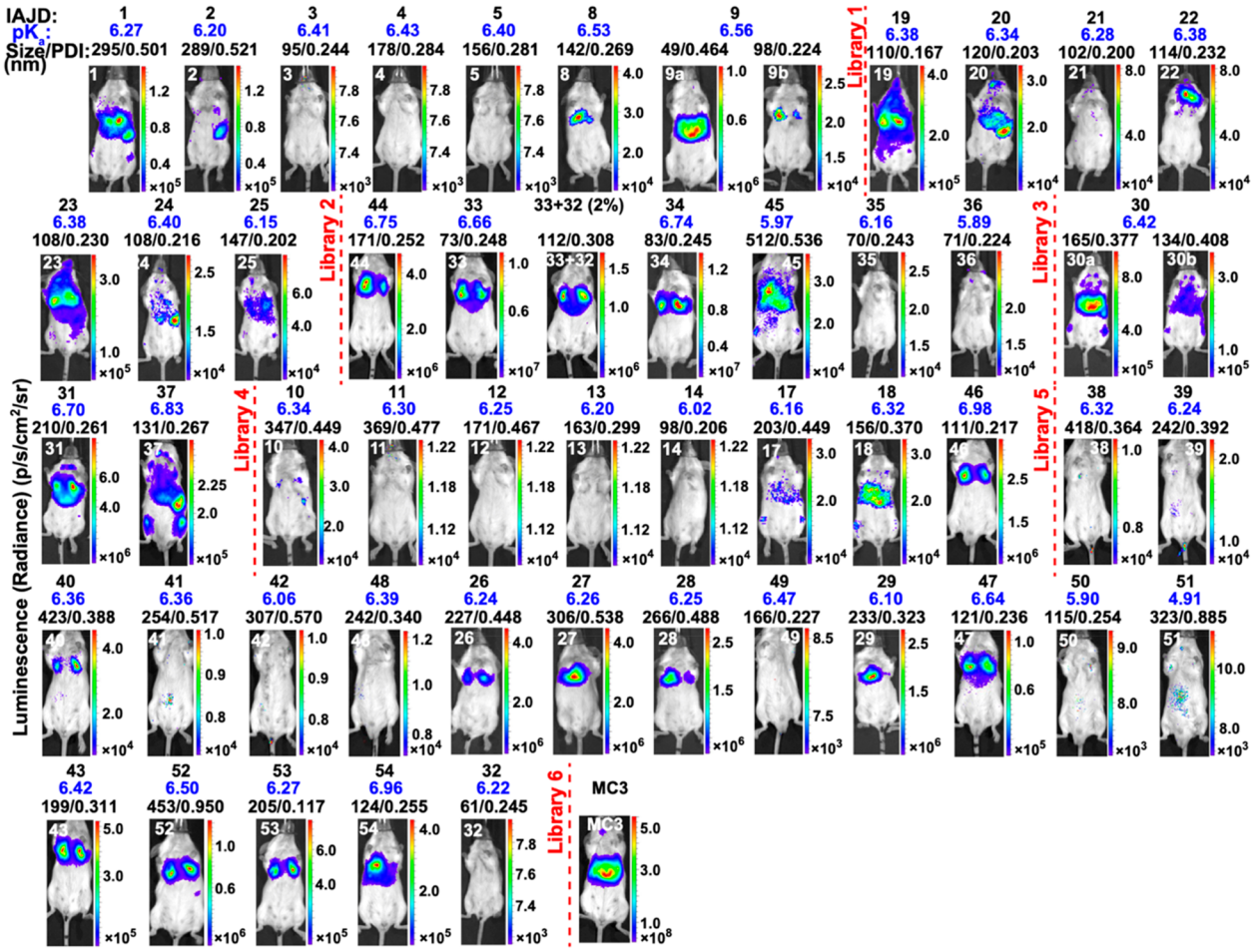

Figure 5. *In vivo* transfection results of DNPs. Details of these experiments are available in Table S7. Diameters and polydispersities of DNPs (both in black) and pK_a values of IAJDs (in blue) are shown under the number of the IAJD molecule. All these data are printed on top of each mouse image. The scale of luminescence values is also shown.

names are presented in Figures S3 (libraries 1, 2, 3, 4), S4 (library 5), and S5 (library 6).

Self-Assembly of DNP Vesicles from IAJDs and of DNPs by Coassembly of IAJDs with mRNA by Simple Injection. The simple injection methodology employed previously for the self-assembly of uniform[12a,c] DSs from JDs[12a,c,13d] and of GDSs from JGDs[13a] with predictable dimensions and narrow PDI was adapted to the self-assembly by injection of a solution of IAJDs and coassembly of IAJDs together with mRNA. Simple injection of an ethanol solution of IAJDs into a neutral buffer such as TRIS produces uniform DNPs with dimensions that are, as in the case of DSs[12a,c,d] and GDSs,[13a] concentration dependent. However, these DNPs are not stable in PBS buffer. Injection of an ethanol solution of IAJD into an acidic citrate or acetate buffer solution of pH 3 to 5.2 containing mRNA resulted in coassembly of IAJD with mRNA into uniform DNPs (Tables S1 to S7, Figures S7 to S19). More than 98% of mRNA is coassembled within the interior of the DNPs (Table S8). These DNPs can be used for *in vitro* and *in vivo* transfection experiments before or after dialysis to pH 7.4. Most of these DNPs are stable at 5 °C for more than 135 days (Table S10, Figure S20) including in serum (Table S11). Analysis of the DNPs without mRNA by cryo-TEM demonstrated that they are vesicles with dimensions and PDIs similar to those determined by DLS (Figure 3). More detailed cryo-TEM data of DNPs without and with mRNA and their analysis will be reported soon.

***In Vitro* Transfection Activity of DNPs in Human Embryonic Kidney (HEK) 293T Cells.** HEK293T cells were seeded into 96-well plates (20 000 cells/well/200 μL) and cultured for 18−20 h at 37 °C in 5% CO_2 complete cell culture media. Screening experiments were performed with non-optimized DNPs containing naked nucleoside-modified mRNA[18] of molar mass 664 341 encoding firefly luciferase (Luc-mRNA). A constant concentration of Luc-mRNA of 125 ng/well was used. The *trans*IT (TransIT-mRNA transfection kit from Mirus Bio) and MC3-based LNPs (MC3: DLin-MC3-DMA, which is an FDA-approved LNP for siRNA delivery)[4a] were used as positive controls for cell transfection at a concentration of Luc-mRNA of 125 ng/well, identical to that of the tested DNPs. Subsequently cells were cultured for 18−20 h, the medium was aspirated under reduced pressure by a glass pipet, and cells were lysed with 30 μL/well of cell culture lysis reagent (Promega). The luminescence intensity corresponding to the luciferase protein expressed was characterized and analyzed.

All 54 IAJDs from Figure 2 were coassembled by injection with mRNA[18] in DNPs and were used in these experiments without dialysis. Tables S1, S2, S3, S4, and S5 summarize the conditions employed for the preparation of the DNPs, their diameter (in nm), and PDI as obtained by DLS experiments

https://doi.org/10.1021/jacs.1c05813
J. Am. Chem. Soc. XXXX, XXX, XXX−XXX

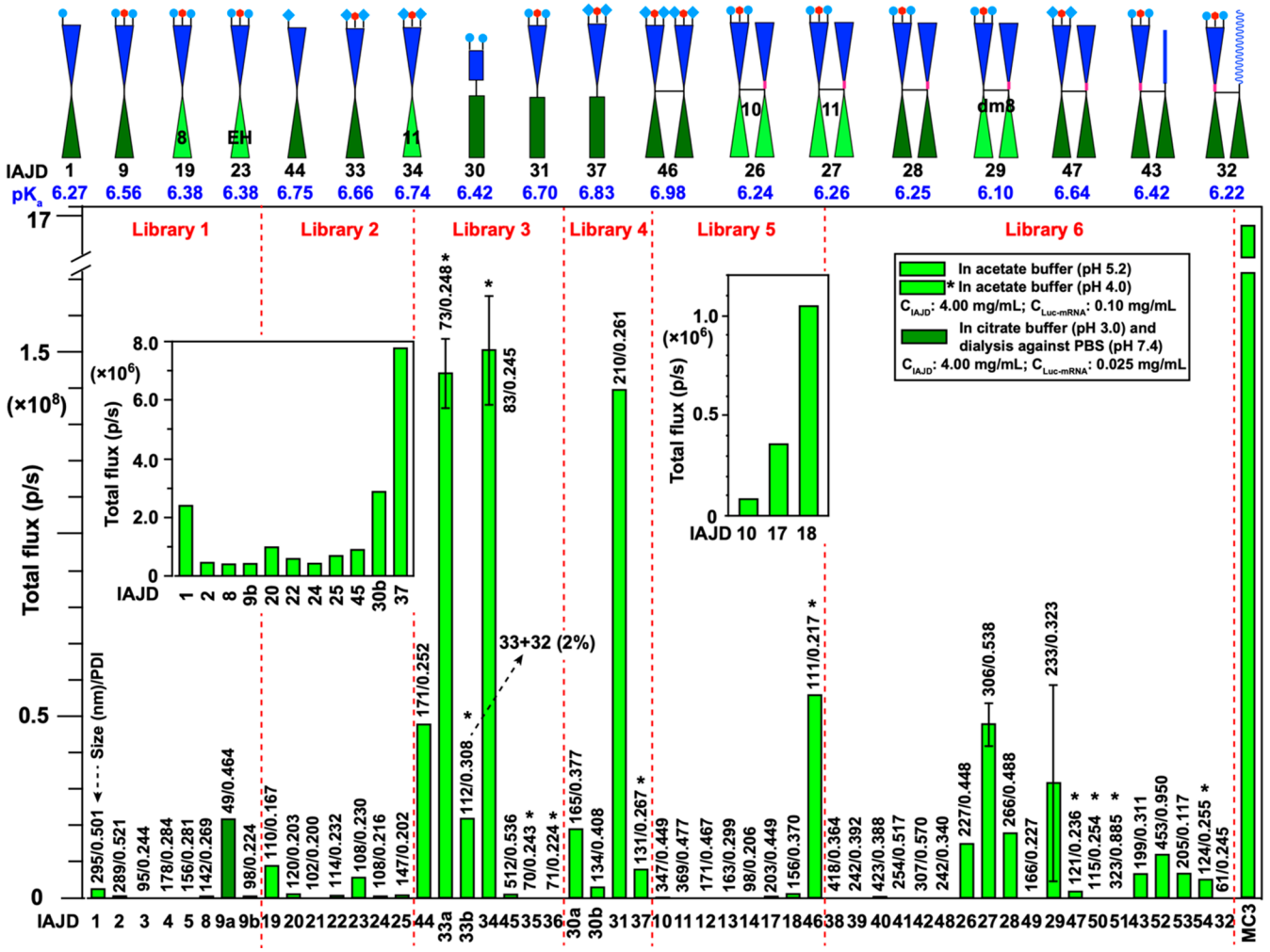

Figure 6. Quantification of luciferase signal from *in vivo* images of Figure 5 and Table S7.

and the luminescence results. Each experiment was performed at least three times. The results from Tables S1 to S5 were combined together with some optimization experiments for IAJD33, IAJD34, IAJD9, and IAJD22 and plotted in the insets in Figure 4. Out of 54 DNPs, 44 (81%) showed activity *in vitro* (Figure 4). Without optimization, two of them, DNP9- and DNP22-based DNPs, display higher activity than the positive controls LNP based on MC3 and *Trans*IT, while four of them, DNP8, DNP9, DNP21, and DNP22, show higher activity than the most commonly used positive control LNP based on MC3.[4]

***In Vivo* mRNA Delivery in Mice with DNPs.** Six- to 8-week-old female or male mice were used in these experiments. Four to 7 h after injection with a 100 μL solution of DNP encapsulated with 10 μg of Luc-mRNA the mice were imaged 10 min after intraperitoneal injection with D-luciferin, 15 mg/mL at 10 μL/g of body weight. The exposure time was 15 s to 1 min. For imaging of the organs, mice were sacrificed, the organs were immediately collected, and bioluminescence imaging was performed. Table S7 summarizes all DNP injection assembly data including *D* in nm and PDI determined by DLS together with the results obtained *in vivo*. Figure 5 shows all mice experiments including the *D* in nm and PDI of DNPs (both in black on top of the mouse image) and the pK_a values of the corresponding IAJDs (in blue also on top of the mouse image) of all compounds used for delivery experiments.

The results from Figures 4 and 5 provide a proof of concept for the one-component multifunctional sequence-defined ionizable amphiphilic Janus dendrimer delivery systems for mRNA even if optimized results are not yet available. The summary of the results from Figure 5 indicates that there seem to be no correlation between the activity of the DNPs *in vivo* and the same experiments *in vitro* (Figure 4). We are not able yet to explain this lack of correlation between *in vitro* and *in vivo* experiments. Although more experiments are required to clarify the dependence between pK_a and activity *in vitro* and *in vivo*, the results from Figure 5 show that the most active IAJD 33, 34, and 31 based DNPs do not have the lowest pK_a values. The results from Figure 5 also demonstrate that there is quite a tolerance of the activity of DNPs to their diameters and polydispersity. Larger than 100 nm diameter DNPs appear to be as active as lower than 100 nm diameter DNPs (Figure 5). However, quantitative correlations for the dependences of activity with pK_a and DNP dimensions must be studied. The stability of the dimension of 40 DNPs was investigated as a function of time at 5 °C. Unoptimized experiments showed that the dimensions of 19 out of 40 DNPs were very stable after being stored at 5 °C for up to 135 days (Figure 7). Almost all these DNPs were assembled from IAJDs containing a benzyl ether in their hydrophilic part (Table S9). A very interesting series of activity trends is observed when the data from Figures 5 and 6 are compared. IAJD9, IAJD22, IAJD33,

https://doi.org/10.1021/jacs.1c05813
J. Am. Chem. Soc. XXXX, XXX, XXX−XXX

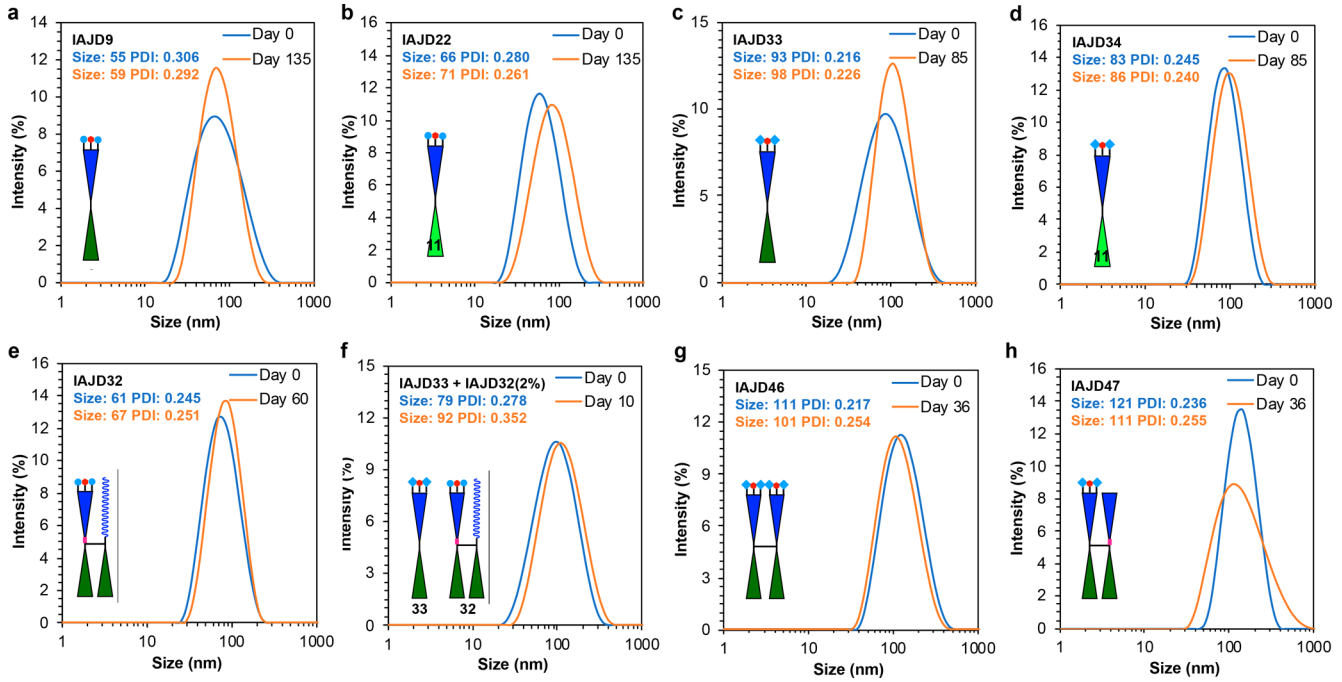

Figure 7. Examples of excellent stability of DNPs assembled from (a) IAJD9; (b) IAJD22; (c) IAJD33; (d) IAJD34; (e) IAJD32; (f) IAJD33+IAJD32 (2%); (g) IAJD46; and (h) IAJD47.

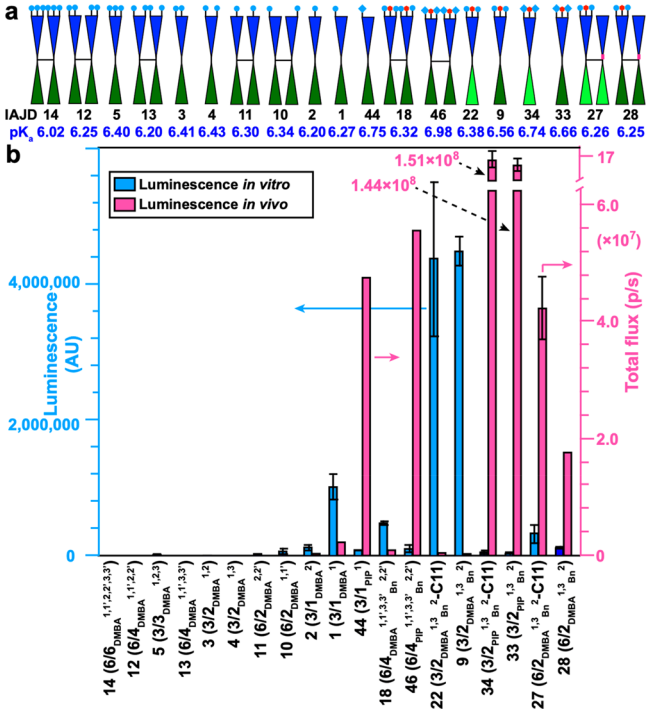

Figure 8. Comparison of the concentration and sequence of the ionizable amines of IAJDs on activity of DNPs *in vitro* and *in vivo*.

and IAJD34 single−single compounds form remarkably stable DNPs that also show high *in vitro* or *in vivo* activity (Figure 6). IAJD46 is the twin−twin of IAJD33. On the other hand, the activity of the DNP46 is about half that of DNP33 (Figures 6 and 7). The hybrid twin-mix IAJD47 is also based on the structure of IAJD33 or half of the structure of IAJD46. However, the activity of the DNP47 is much lower than that of both DNP33 and DNP46. Even more interesting is the comparison of single−single IAJD9 with the hybrid twin-mix IAJD32 (Figures 6 and 7).

Figure 6 plots the results from Figure 5. Without any optimization, out of the 54 DNPs investigated, 31 (57%) show activity *in vivo*. Two of them, DNP33 and DNP34, demonstrated very high activity in the lung. Single−single IAJD9-derived DNP9 exhibits good activity (Figure 6) and stability (Figure 7). At the same time the corresponding hybrid twin-mix IAJD32-based DNP32 derived from IAJD9 and a single PEG of degree of polymerization 45 (Figure 2) also exhibits excellent stability (Figure 7) but is completely inactive in mice (Figure 6). In order to clarify this result, we prepared several coassembled DNPs based on very active IAJDs and a small concentration of IAJD32. One example is the DNP assembled from IAJD33 and 2% IAJD32 (compare Figure 7f with Figure 6). The stability of this combined DNP is excellent (Figure 7f) and is comparable with that of DNP32 assembled from IAJD32 alone. However, the *in vivo* activity of DNP coassembled from IAJD33 with 2% IAJD32 is only a small fraction of the activity of the DNP33 (Figure 6). This trend confirms the reports on the PEG interfering with cellular uptake known as the "PEG dilemma".[8] Therefore, while the insertion of a small fraction of PEG conjugated to an IAJD can dramatically increase the stability of the resulting DNP, it also decreases even more dramatically its activity *in vivo*. Incorporation of short groups of oligooxyethylene with different degrees of polymerization (DP) and chain ends[12] or carbohydrate[13] fragments in the structure of single−single, twin−twin, or even hybrid twin-mix IAJDs could provide a solution to this problem. Research along this line with PEG of DP = 3, 4, 8, 12, 18, 22, and 45 and with lactose[13a,d] is in progress. Some preliminary data performed with DNP9, DNP43 (DP = 3), DNP52 (DP = 4), DNP53 (DP = 8), and DNP32 (DP = 45) (Figure 2) indicate, before optimization, a decrease followed by an increase and subsequently another decrease of the *in vivo* activity when

https://doi.org/10.1021/jacs.1c05813
J. Am. Chem. Soc. XXXX, XXX, XXX−XXX

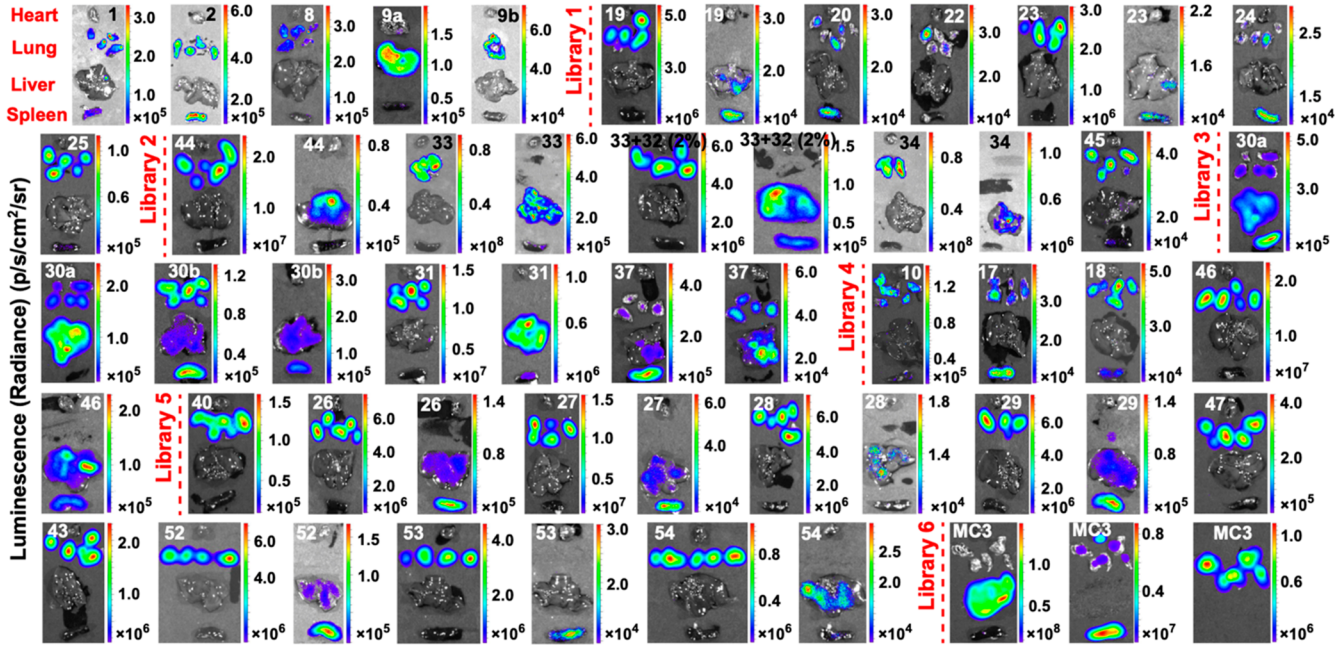

Figure 9. Images of the mice organs from the *in vivo* experiments presented in Figure 5.

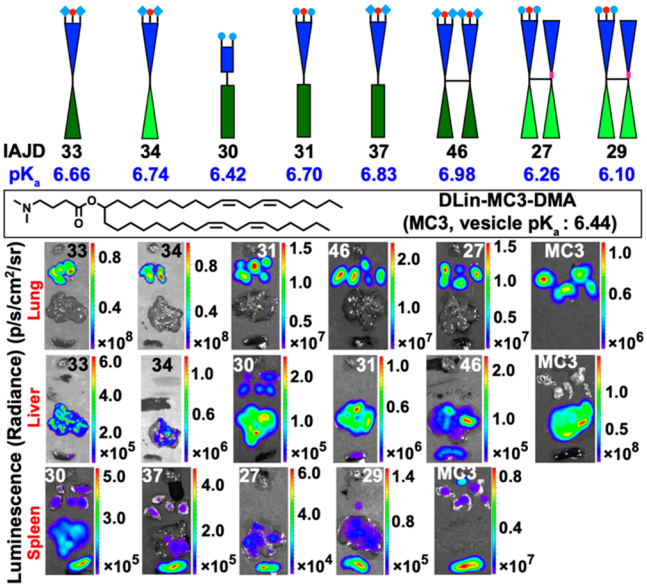

Figure 10. Representative images of mRNA delivery to different organs by one-component DNPs.

DP of PEG increases in the hybrid twin-mix architecture of IADSs (Figure 2).

The Role of Ionizable Amine Concentration and Sequence on the Activity of the Corresponding DNPs. We demonstrated that the binding activity of sugars located on the surface of the GDSs assembled from amphiphilic JGDs toward sugar-binding proteins increases by decreasing the concentration of the sugar in a sequence-defined process.[12b−f] This unexpected trend was explained by self-organization, on the periphery of the GDSs, leading to a morphology that facilitated higher binding activity between the sugar and the proteins at lower concentrations of sugar (Figure S33).[13d,f]

Figure 8 plots representative activity data for the sequence-defined IAJD-derived DNPs for both *in vitro* and *in vivo* experiments. Low or no activity was observed at high concentrations of ionizable amines in the structure of the IAJD, and extremely high activities were observed at lower ionizable amine concentration in very specific sequences. Without discussing in great detail, the results from Figure 8 provide a mechanism to engineer the activity of DNPs via the sequence and concentration of their ionizable amines. The change in activity observed in Figure 8 is much higher than that observed in the case of sequence-defined dendrimersomes (Figure 2 from ref 13d shown in Figure S33).[12d]

Some Comments on Potential Targeted Delivery of mRNA and Reproducibility of *in Vitro* and *in Vivo* Transfection Experiments. Figures 9 and 10 summarize representative organ delivery data selected from the experiments reported in Figure 5. They illustrate the luminescence intensity reflecting delivery activity in the heart, lung, liver, and spleen as a function of the structure of the IAJD employed in the design of the structure of the DNP used in the delivery of mRNA. The highest luminescence is exhibited by single−single IAJD33 and IAJD34 forming DNPs (10^8) in the lung. The next highest is based on the IAJD31, IAJD46, and IAJD27 (10^7) DNPs and is also in the lung.

These lung activities are higher than the activity in the lung of the control experiment with LNP based on the FDA-approved MC3 (Figure 10). It is important to realize that organ activities from Figure 10 are much higher than overall mouse activities from Figures 6 and 9. The next higher activity is in the liver (Figures 9 and 10). Without optimization, the luminescence in the liver is 10^6 for IAJD31- and IAJD34-based DNPs and 10^5 for IAJD30-, IAJD33-, and IAJD46-based DNPs. They are smaller than the values of the MC3-based control experiment, which is 10^8. The highest activity in the spleen is for IAJD29-, IAJD30-, and IAJD37-based DNPs (10^5) and IAJD27-based DNP (10^4). The control experiment with MC3-based LNP is 10^7 in the spleen. Notably, dendrimersome nanoparticles self-organized from twin−twin and single−single JDs without ionizable amines, and mRNA and IAJD1 and IAJD9 are distributed *in vivo* to all organs with higher distribution in the liver especially for twin−twin JD and IAJD9

https://doi.org/10.1021/jacs.1c05813
J. Am. Chem. Soc. XXXX, XXX, XXX−XXX

(Figure S34). The most active DNPs were tested both *in vitro* (Figure 4) and *in vivo* (Figure 6) up to six times. Excellent reproducibility was obtained in all cases except for DNP9, which shows very good reproducibility *in vitro* but poor reproducibility *in vivo*. Experiments are in progress to elucidate this issue. The results reported here indicate that one-component IAJDs could also provide a potential strategy to target different organs.

CONCLUSIONS

The design and accelerated modular-orthogonal synthesis of six libraries containing 54 multifunctional sequence-defined ionizable amphiphilic Janus dendrimers are reported. All 54 IAJDs coassemble with mRNA by simple injection in acidic buffers to generate dendrimersome nanoparticles with predictable dimensions and narrow polydispersity. The dimensions of these DNPs are stable for over 135 days at 5 °C. Among the 54 DNPs encapsulating Luciferase-mRNA, 44 (81%) showed activity *in vitro* and four of them showed higher activity than the four-component lipid nanoparticles obtained from the FDA-approved MC3 control experiment. Thirty one (57%) DNPs displayed activity *in vivo*, with two of them exhibiting higher activity than the MC3 control experiment in the lung. This lung activity is exceptional for synthetic delivery of mRNA and could be, according to our knowledge, one of the highest demonstrated thus far.[19] These unoptimized preliminary experiments provide proof of concept for the one-component multifunctional sequence-defined amphiphilic Janus dendrimer as an efficient delivery system for mRNA. Just like in the case of sequence-defined GDSs (Figure S33), this one-component delivery platform is more active at low ionizable amine concentration incorporated in a suitable sequence-defined arrangement (Figure 8). These sequence-defined IAJDs and DNPs will be employed to elucidate the mechanisms of encapsulation and release of mRNA from supramolecular virus-like assemblies and for the production of vaccines and drugs. It is expected that their ionizable amine fragments may not be able to segregate in the center of their DNPs, as they do in the case of LNPs. Finally but importantly, the DNPs reported here represent some of the most interesting and challenging hybrid natural−synthetic complex systems[20] with numerous potential applications in health sciences.

ASSOCIATED CONTENT

Supporting Information

The Supporting Information is available free of charge at https://pubs.acs.org/doi/10.1021/jacs.1c05813.

Experimental methods, synthesis, and characterization of all 54 IAJDs, dimensions and polydispersities, *in vitro* and *in vivo* transfection data of DNPs, DLS curves of DNPs, stability characterization of DNPs, pK_a measurements, and supplemental references (PDF)

AUTHOR INFORMATION

Corresponding Authors

Drew Weissman − *Department of Medicine, Perelman School of Medicine, University of Pennsylvania, Philadelphia, Pennsylvania 19104, United States;* orcid.org/0000-0002-1501-6510; Email: dreww@pennmedicine.upenn.edu

Virgil Percec − *Roy & Diana Vagelos Laboratories, Department of Chemistry, University of Pennsylvania, Philadelphia, Pennsylvania 19104-6323, United States;* orcid.org/0000-0001-5926-0489; Email: percec@sas.upenn.edu

Authors

Dapeng Zhang − *Roy & Diana Vagelos Laboratories, Department of Chemistry, University of Pennsylvania, Philadelphia, Pennsylvania 19104-6323, United States;* orcid.org/0000-0003-4222-6107

Elena N. Atochina-Vasserman − *Department of Medicine, Perelman School of Medicine, University of Pennsylvania, Philadelphia, Pennsylvania 19104, United States*

Devendra S. Maurya − *Roy & Diana Vagelos Laboratories, Department of Chemistry, University of Pennsylvania, Philadelphia, Pennsylvania 19104-6323, United States;* orcid.org/0000-0002-4488-9927

Ning Huang − *Roy & Diana Vagelos Laboratories, Department of Chemistry, University of Pennsylvania, Philadelphia, Pennsylvania 19104-6323, United States;* orcid.org/0000-0001-8874-3439

Qi Xiao − *Roy & Diana Vagelos Laboratories, Department of Chemistry, University of Pennsylvania, Philadelphia, Pennsylvania 19104-6323, United States;* orcid.org/0000-0002-6470-0407

Nathan Ona − *Department of Medicine, Perelman School of Medicine, University of Pennsylvania, Philadelphia, Pennsylvania 19104, United States;* orcid.org/0000-0002-8729-2223

Matthew Liu − *Roy & Diana Vagelos Laboratories, Department of Chemistry, University of Pennsylvania, Philadelphia, Pennsylvania 19104-6323, United States;* orcid.org/0000-0002-5004-9182

Hamna Shahnawaz − *Department of Medicine, Perelman School of Medicine, University of Pennsylvania, Philadelphia, Pennsylvania 19104, United States*

Houping Ni − *Department of Medicine, Perelman School of Medicine, University of Pennsylvania, Philadelphia, Pennsylvania 19104, United States*

Kyunghee Kim − *Department of Materials Science & Engineering, University of Delaware, Newark, Delaware 19716, United States;* orcid.org/0000-0002-4549-0686

Margaret M. Billingsley − *Department of Bioengineering, University of Pennsylvania, Philadelphia, Pennsylvania 19104-6321, United States;* orcid.org/0000-0003-4499-9066

Darrin J. Pochan − *Department of Materials Science & Engineering, University of Delaware, Newark, Delaware 19716, United States;* orcid.org/0000-0002-0454-2339

Michael J. Mitchell − *Department of Bioengineering, University of Pennsylvania, Philadelphia, Pennsylvania 19104-6321, United States;* orcid.org/0000-0002-3628-2244

Complete contact information is available at: https://pubs.acs.org/10.1021/jacs.1c05813

Author Contributions

♦D.Z. and E.N.A.-V. contributed equally to this work.

Notes

The authors declare no competing financial interest.

https://doi.org/10.1021/jacs.1c05813
J. Am. Chem. Soc. XXXX, XXX, XXX−XXX

■ ACKNOWLEDGMENTS

This work was supported by National Science Foundation Grants DMR-1807127, DMR-1720530, and DMR-2104554, the P. Roy Vagelos Chair at the University of Pennsylvania, and the Alexander von Humboldt Foundation (all to V.P.). NMR Instrumentation (NEO400) was supported by the NSF Major Research Instrumentation Program (award NSF CHE-1827457) and Vagelos Institute for Energy Science and Technology. M.J.M. acknowledges support from a Burroughs Wellcome Fund Career Award at the Scientific Interface (CASI) and a U.S. National Institutes of Health (NIH) Director's New Innovator Award (DP2 TR002776). D.W. and E.A.N.-V. were funded by NIH grants (AI124429 and 1UM1-AI144371). The authors also thank the Professor Karen I. Goldberg laboratory at Penn for access to pH instrumentation.

■ REFERENCES

(1) (a) Luo, D.; Saltzman, W. M. Synthetic DNA Delivery Systems. *Nat. Biotechnol.* **2000**, *18*, 33−37. (b) Thomas, C. E.; Ehrhardt, A.; Kay, M. A. Progress and Problems with the Use of Viral Vectors for Gene Therapy. *Nat. Rev. Genet.* **2003**, *4*, 346−358. (c) Peer, D.; Karp, J. M.; Hong, S.; Farokhzad, O. C.; Margalit, R.; Langer, R. Nanocarriers as an Emerging Platform for Cancer Therapy. *Nat. Nanotechnol.* **2007**, *2*, 751−760. (d) Whitehead, K. A.; Langer, R.; Anderson, D. G. Knocking down Barriers: Advances in SiRNA Delivery. *Nat. Rev. Drug Discovery* **2009**, *8*, 129−138. (e) Cullis, P. R.; Hope, M. J. Lipid Nanoparticle Systems for Enabling Gene Therapies. *Mol. Ther.* **2017**, *25*, 1467−1475. (f) Ramamoorth, M.; Narvekar, A. Non Viral Vectors in Gene Therapy- an Overview. *J. Clin. Diagn. Res.* **2015**, *9*, GE01−06. (g) Wickham, T. J. Ligand-Directed Targeting of Genes to the Site of Disease. *Nat. Med.* **2003**, *9*, 135−139. (h) Hajj, K. A.; Whitehead, K. A. Tools for Translation: Non-Viral Materials for Therapeutic mRNA Delivery. *Nat. Rev. Mater.* **2017**, *2*, 1−17. (i) Reichmuth, A. M.; Oberli, M. A.; Jaklenec, A.; Langer, R.; Blankschtein, D. mRNA Vaccine Delivery Using Lipid Nanoparticles. *Ther. Delivery* **2016**, *7*, 319−334. (j) Kauffman, K. J.; Webber, M. J.; Anderson, D. G. Materials for Non-Viral Intracellular Delivery of Messenger RNA Therapeutics. *J. Controlled Release* **2016**, *240*, 227−234. (k) Pardi, N.; Hogan, M. J.; Porter, F. W.; Weissman, D. mRNA Vaccines — a New Era in Vaccinology. *Nat. Rev. Drug Discovery* **2018**, *17*, 261−279. (l) Buschmann, M. D.; Carrasco, M. J.; Alishetty, S.; Paige, M.; Alameh, M. G.; Weissman, D. Nanomaterial Delivery Systems for mRNA Vaccines. *Vaccines* **2021**, *9*, 65. (m) Wilson, J. M. Genetic Diseases, Immunology, Viruses, and Gene Therapy. *Hum. Gene Ther.* **2014**, *25*, 257−261. (n) Cross, R. The Redemption of James Wilson, Gene Therapy Pioneer. *C&EN* **2019**, *97*, 26. (o) Nguyen, J.; Szoka, F. C. Nucleic Acid Delivery: The Missing Pieces of the Puzzle? *Acc. Chem. Res.* **2012**, *45*, 1152−1162. (p) Reinhard, K.; Rengstl, B.; Oehm, P.; Michel, K.; Billmeier, A.; Hayduk, N.; Klein, O.; Kuna, K.; Ouchan, Y.; Wöll, S.; Christ, E.; Weber, D.; Suchan, M.; Bukur, T.; Birtel, M.; Jahndel, V.; Mroz, K.; Hobohm, K.; Kranz, L.; Diken, M.; Kühlcke, K.; Türeci, Ö.; Sahin, U. An RNA Vaccine Drives Expansion and Efficacy of Claudin-CAR-T Cells Against Solid Tumors. *Science* **2020**, *367*, 446−453. (q) Sabnis, S.; Kumarasinghe, E. S.; Salerno, T.; Mihai, C.; Ketova, T.; Senn, J. J.; Lynn, A.; Bulychev, A.; McFadyen, I.; Chan, J.; Almarsson, Ö.; Stanton, M. G.; Benenato, K. E. A Novel Amino Lipid Series for mRNA Delivery: Improved Endosomal Escape and Sustained Pharmacology and Safety in Non-human Primates. *Mol. Ther.* **2018**, *26*, 1509−1519. (r) Miyata, K.; Nishiyama, N.; Kataoka, K. Rational Design of Smart Supramolecular Assemblies for Gene Delivery: Chemical Challenges in the Creation of Artificial Viruses. *Chem. Soc. Rev.* **2012**, *41*, 2562−2574. (s) Cabral, H.; Kinoh, H.; Kataoka, K. Tumor-Targeted Nanomedicine for Immunotherapy. *Acc. Chem. Res.* **2020**, *53*, 2765−2776. (t) Li, J.; Kataoka, K. Chemo-Physical Strategies to Advance the in Vivo Functionality of Targeted Nanomedicine: The Next Generation. *J. Am. Chem. Soc.* **2021**, *143*, 538−559. (u) Heredia, K. L.; Nguyen, T. H.; Chang, C.-W.; Bulmus, V.; Davis, T. P.; Maynard, H. D. Reversible siRNA-Polymer Conjugates by RAFT Polymerization. *Chem. Commun.* **2008**, 3245−3247. (v) Deng, Z. J.; Morton, S. W.; Ben-Akiva, E.; Dreaden, E. C.; Shopsowitz, K. E.; Hammond, P. T. Layer-by-Layer Nanoparticles for Systemic Codelivery of an Anticancer Drug and siRNA for Potential Triple-Negative Breast Cancer Treatment. *ACS Nano* **2013**, *7*, 9571−9584. (w) Lacroix, A.; Sleiman, H. F. DNA Nanostructures: Current Challenges and Opportunities for Cellular Delivery. *ACS Nano* **2021**, *15*, 3631−3645. (x) Billingsley, M. M.; Singh, N.; Ravikumar, P.; Zhang, R.; June, C. H.; Mitchell, M. J. Ionizable Lipid Nanoparticle-Mediated mRNA Delivery for Human CAR T Cell Engineering. *Nano Lett.* **2020**, *20*, 1578−1589. (y) Riley, R. S.; Kashyap, M. V.; Billingsley, M. M.; White, B.; Alameh, M.-G.; Bose, S. K.; Zoltick, P. W.; Li, H.; Zhang, R.; Cheng, A. Y.; Weissman, D.; Peranteau, W. H.; Mitchell, M. J. Ionizable Lipid Nanoparticles for in Utero mRNA Delivery. *Sci. Adv.* **2021**, *7*, No. eaba1028. (z) Chahal, J. S.; Khan, O. F.; Cooper, C. L.; McPartlan, J. S.; Tsosie, J. K.; Tilley, L. D.; Sidik, S. M.; Lourido, S.; Langer, R.; Bavari, S.; Ploegh, H. L.; Anderson, D. G. Dendrimer-RNA Nanoparticles Generate Protective Immunity Against Lethal Ebola, H1N1 Influenza, and *Toxoplasma Gondii* Challenges with a Single Dose. *Proc. Natl. Acad. Sci. U. S. A.* **2016**, *113*, E4133−E4142.

(2) (a) Baum, C.; Kustikova, O.; Modlich, U.; Li, Z.; Fehse, B. Mutagenesis and Oncogenesis by Chromosomal Insertion of Gene Transfer Vectors. *Hum. Gene Ther.* **2006**, *17*, 253−263. (b) Bessis, N.; GarciaCozar, F. J.; Boissier, M.-C. Immune Responses to Gene Therapy Vectors: Influence on Vector Function and Effector Mechanisms. *Gene Ther.* **2004**, *11*, S10−S17. (c) Bouard, D.; Alazard-Dany, D.; Cosset, F.-L. Viral Vectors: From Virology to Transgene Expression. *Br. J. Pharmacol.* **2009**, *157*, 153−165.

(3) (a) Esfand, R.; Tomalia, D. A. Poly(Amidoamine) (PAMAM) Dendrimers: From Biomimicry to Drug Delivery and Biomedical Applications. *Drug Discovery Today* **2001**, *6*, 427−436. (b) Svenson, S.; Tomalia, D. A. Dendrimers in Biomedical Applications–Reflections on the Field. *Adv. Drug Delivery Rev.* **2005**, *57*, 2106−2129. (c) Kukowska-Latallo, J. F.; Bielinska, A. U.; Johnson, J.; Spindler, R.; Tomalia, D. A.; Baker, J. R. Efficient Transfer of Genetic Material into Mammalian Cells Using Starburst Polyamidoamine Dendrimers. *Proc. Natl. Acad. Sci. U. S. A.* **1996**, *93*, 4897−4902. (d) Mintzer, M. A.; Simanek, E. E. Nonviral Vectors for Gene Delivery. *Chem. Rev.* **2009**, *109*, 259−302. (e) Palmerston Mendes, L.; Pan, J.; Torchilin, V. P. Dendrimers as Nanocarriers for Nucleic Acid and Drug Delivery in Cancer Therapy. *Molecules* **2017**, *22*, 1401. (f) Khan, O. F.; Zaia, E. W.; Jhunjhunwala, S.; Xue, W.; Cai, W.; Yun, D. S.; Barnes, C. M.; Dahlman, J. E.; Dong, Y.; Pelet, J. M.; Webber, M. J.; Tsosie, J. K.; Jacks, T. E.; Langer, R.; Anderson, D. G. Dendrimer-Inspired Nanomaterials for the in Vivo Delivery of siRNA to Lung Vasculature. *Nano Lett.* **2015**, *15*, 3008−3016. (g) Khan, O. F.; Zaia, E. W.; Yin, H.; Bogorad, R. L.; Pelet, J. M.; Webber, M. J.; Zhuang, I.; Dahlman, J. E.; Langer, R.; Anderson, D. G. Ionizable Amphiphilic Dendrimer-Based Nanomaterials with Alkyl-Chain-Substituted Amines for Tunable siRNA Delivery to the Liver Endothelium In Vivo. *Angew. Chem., Int. Ed.* **2014**, *53*, 14397−14401. (h) Guillot-Nieckowski, M.; Eisler, S.; Diederich, F. Dendritic Vectors for Gene Transfection. *New J. Chem.* **2007**, *31*, 1111−1127. (i) Guillot, M.; Eisler, S.; Weller, K.; Merkle, H. P.; Gallani, J.-L.; Diederich, F. Effects of Structural Modification on Gene Transfection and Self-Assembling Properties of Amphiphilic Dendrimers. *Org. Biomol. Chem.* **2006**, *4*, 766−769. (j) Meyer, E. A.; Castellano, R. K.; Diederich, F. Interactions with Aromatic Rings in Chemical and Biological Recognition. *Angew. Chem., Int. Ed.* **2003**, *42*, 1210−1250. (k) Liu, X.; Zhou, J.; Yu, T.; Chen, C.; Cheng, Q.; Sengupta, K.; Huang, Y.; Li, H.; Liu, C.; Wang, Y.; Posocco, P.; Wang, M.; Cui, Q.; Giorgio, S.; Fermeglia, M.; Qu, F.; Pricl, S.; Shi, X.; Liang, Z.; Rocchi, P.; Rossi, J. J.; Peng, L. Adaptive Amphiphilic Dendrimer-Based Nanoassemblies as Robust and Versatile siRNA Delivery Systems. *Angew. Chem., Int. Ed.* **2014**, *53*, 11822−11827. (l) Dong, Y.; Yu, T.; Ding, L.; Laurini, E.; Huang, Y.; Zhang, M.; Weng, Y.; Lin, S.; Chen,

https://doi.org/10.1021/jacs.1c05813
J. Am. Chem. Soc. XXXX, XXX, XXX−XXX

P.; Marson, D.; Jiang, Y.; Giorgio, S.; Pricl, S.; Liu, X.; Rocchi, P.; Peng, L. A Dual Targeting Dendrimer-Mediated siRNA Delivery System for Effective Gene Silencing in Cancer Therapy. *J. Am. Chem. Soc.* **2018**, *140*, 16264−16274.

(4) (a) Jayaraman, M.; Ansell, S. M.; Mui, B. L.; Tam, Y. K.; Chen, J.; Du, X.; Butler, D.; Eltepu, L.; Matsuda, S.; Narayanannair, J. K.; Rajeev, K. G.; Hafez, I. M.; Akinc, A.; Maier, M. A.; Tracy, M. A.; Cullis, P. R.; Madden, T. D.; Manoharan, M.; Hope, M. J. Maximizing the Potency of siRNA Lipid Nanoparticles for Hepatic Gene Silencing In Vivo. *Angew. Chem., Int. Ed.* **2012**, *51*, 8529−8533. (b) Kulkarni, J. A.; Witzigmann, D.; Chen, S.; Cullis, P. R.; van der Meel, R. Lipid Nanoparticle Technology for Clinical Translation of siRNA Therapeutics. *Acc. Chem. Res.* **2019**, *52*, 2435−2444.

(5) Allen, T. M.; Cullis, P. R. Drug Delivery Systems: Entering the Mainstream. *Science* **2004**, *303*, 1818−1822.

(6) (a) Chen, D.; Love, K. T.; Chen, Y.; Eltoukhy, A. A.; Kastrup, C.; Sahay, G.; Jeon, A.; Dong, Y.; Whitehead, K. A.; Anderson, D. G. Rapid Discovery of Potent Sirna-Containing Lipid Nanoparticles Enabled by Controlled Microfluidic Formulation. *J. Am. Chem. Soc.* **2012**, *134*, 6948−6951. (b) Zhigaltsev, I. V.; Belliveau, N.; Hafez, I.; Leung, A. K.; Huft, J.; Hansen, C.; Cullis, P. R. Bottom-up Design and Synthesis of Limit Size Lipid Nanoparticle Systems with Aqueous and Triglyceride Cores Using Millisecond Microfluidic Mixing. *Langmuir* **2012**, *28*, 3633−3640. (c) Leung, A. K.; Hafez, I. M.; Baoukina, S.; Belliveau, N. M.; Zhigaltsev, I. V.; Afshinmanesh, E.; Tieleman, D. P.; Hansen, C. L.; Hope, M. J.; Cullis, P. R. Lipid Nanoparticles Containing Sirna Synthesized by Microfluidic Mixing Exhibit an Electron-Dense Nanostructured Core. *J. Phys. Chem. C* **2012**, *116*, 18440−18450. (d) Leung, A. K.; Tam, Y. Y.; Chen, S.; Hafez, I. M.; Cullis, P. R. Microfluidic Mixing: A General Method for Encapsulating Macromolecules in Lipid Nanoparticle Systems. *J. Phys. Chem. B* **2015**, *119*, 8698−8706.

(7) (a) Ramezanpour, M.; Schmidt, M. L.; Bodnariuc, I.; Kulkarni, J. A.; Leung, S. S. W.; Cullis, P. R.; Thewalt, J. L.; Tieleman, D. P. Ionizable Amino Lipid Interactions with POPC: Implications for Lipid Nanoparticle Function. *Nanoscale* **2019**, *11*, 14141−14146. (b) Kulkarni, J. A.; Darjuan, M. M.; Mercer, J. E.; Chen, S.; van der Meel, R.; Thewalt, J. L.; Tam, Y. Y. C.; Cullis, P. R. On the Formation and Morphology of Lipid Nanoparticles Containing Ionizable Cationic Lipids and siRNA. *ACS Nano* **2018**, *12*, 4787−4795.

(8) (a) Hatakeyama, H.; Akita, H.; Harashima, H. A Multifunctional Envelope Type Nano Device (MEND) for Gene Delivery to Tumours Based on the EPR Effect: A Strategy for Overcoming the PEG Dilemma. *Adv. Drug Delivery Rev.* **2011**, *63*, 152−160. (b) Sato, Y.; Hatakeyama, H.; Sakurai, Y.; Hyodo, M.; Akita, H.; Harashima, H. A pH-Sensitive Cationic Lipid Facilitates the Delivery of Liposomal siRNA and Gene Silencing Activity in Vitro and in Vivo. *J. Controlled Release* **2012**, *163*, 267−276. (c) Choi, J. S.; MacKay, J. A.; Szoka, F. C. Low-pH-Sensitive PEG-Stabilized Plasmid-Lipid Nanoparticles: Preparation and Characterization. *Bioconjugate Chem.* **2003**, *14*, 420−429. (d) Pelegri-O'Day, E. M.; Lin, E.-W.; Maynard, H. D. Therapeutic Protein-Polymer Conjugates: Advancing Beyond PEGylation. *J. Am. Chem. Soc.* **2014**, *136*, 14323−14332. (e) Whitfield, C. J.; Zhang, M.; Winterwerber, P.; Wu, Y.; Ng, D. Y. W.; Weil, T. Functional DNA-Polymer Conjugates. *Chem. Rev.* **2021**, DOI: 10.1021/acs.chemrev.0c01074.

(9) (a) McKinlay, C. J.; Vargas, J. R.; Blake, T. R.; Hardy, J. W.; Kanada, M.; Contag, C. H.; Wender, P. A.; Waymouth, R. M. Charge-Altering Releasable Transporters (CARTs) for the Delivery and Release of mRNA in Living Animals. *Proc. Natl. Acad. Sci. U. S. A.* **2017**, *114*, E448−E456. (b) McKinlay, C. J.; Benner, N. L.; Haabeth, O. A.; Waymouth, R. M.; Wender, P. A. Enhanced mRNA Delivery into Lymphocytes Enabled by Lipid-Varied Libraries of Charge-Altering Releasable Transporters. *Proc. Natl. Acad. Sci. U. S. A.* **2018**, *115*, E5859−E5866. (c) Benner, N. L.; McClellan, R. L.; Turlington, C. R.; Haabeth, O. A. W.; Waymouth, R. M.; Wender, P. A. Oligo(Serine Ester) Charge-Altering Releasable Transporters: Organocatalytic Ring-Opening Polymerization and Their Use for in Vitro and in Vivo mRNA Delivery. *J. Am. Chem. Soc.* **2019**, *141*, 8416−8421. (d) Blake, T. R.; Ho, W. C.; Turlington, C. R.; Zang, X.; Huttner, M. A.; Wender, P. A.; Waymouth, R. M. Synthesis and Mechanistic Investigations of pH-Responsive Cationic Poly-(Aminoester)s. *Chem. Sci.* **2020**, *11*, 2951−2966. (e) Gillies, E. R.; Fréchet, J. M. J. Dendrimers and Dendritic Polymers in Drug Delivery. *Drug Discovery Today* **2005**, *10*, 35−43.

(10) (a) Bangham, A. D.; Standish, M. M.; Watkins, J. C. Diffusion of Univalent Ions across the Lamellae of Swollen Phospholipids. *J. Mol. Biol.* **1965**, *13*, 238−252. (b) Guo, X.; Szoka, F. C., Jr. Chemical Approaches to Triggerable Lipid Vesicles for Drug and Gene Delivery. *Acc. Chem. Res.* **2003**, *36*, 335−341. (c) Ringsdorf, H.; Schlarb, B.; Venzmer, J. Molecular Architecture and Function of Polymeric Oriented Systems: Models for the Study of Organization, Surface Recognition, and Dynamics of Biomembranes. *Angew. Chem., Int. Ed. Engl.* **1988**, *27*, 113−158. (d) Brea, R. J.; Hardy, M. D.; Devaraj, N. K. Towards Self-Assembled Hybrid Artificial Cells: Novel Bottom-Up Approaches to Functional Synthetic Membranes. *Chem. - Eur. J.* **2015**, *21*, 12564−12570. (e) Thomas, J. L.; Tirrell, D. A. Polyelectrolyte-Sensitized Phospholipid Vesicles. *Acc. Chem. Res.* **1992**, *25*, 336−342. (f) Kunitake, T.; Okahata, Y. A Totally Synthetic Bilayer Membrane. *J. Am. Chem. Soc.* **1977**, *99*, 3860−3861. (g) Kunitake, T. Synthetic Bilayer Membranes: Molecular Design, Self-Organization, and Application. *Angew. Chem., Int. Ed. Engl.* **1992**, *31*, 709−726. (h) Khanal, S.; Brea, R. J.; Burkart, M. D.; Devaraj, N. K. Chemoenzymatic Generation of Phospholipid Membranes Mediated by Type I Fatty Acid Synthase. *J. Am. Chem. Soc.* **2021**, *143*, 8533−8537. (i) Tu, Y.; Peng, F.; Adawy, A.; Men, Y.; Abdelmohsen, L. K. E. A.; Wilson, D. A. Mimicking the Cell: Bio-Inspired Functions of Supramolecular Assemblies. *Chem. Rev.* **2016**, *116*, 2023−2078. (j) Thota, B. N. S.; Urner, L. H.; Haag, R. Supramolecular Architectures of Dendritic Amphiphiles in Water. *Chem. Rev.* **2016**, *116*, 2079−2102. (k) Weiss, M.; Frohnmayer, J. P.; Benk, L. T.; Haller, B.; Janiesch, J.-W.; Heitkamp, T.; Börsch, M.; Lira, R. B.; Dimova, R.; Lipowsky, R.; Bodenschatz, E.; Baret, J.-C.; Vidakovic-Koch, T.; Sundmacher, K.; Platzman, I.; Spatz, J. P. Sequential Bottom-up Assembly of Mechanically Stabilized Synthetic Cells by Microfluidics. *Nat. Mater.* **2018**, *17*, 89−96. (l) Zou, Y.; Henry, W. S.; Ricq, E. L.; Graham, E. T.; Phadnis, V. V.; Maretich, P.; Paradkar, S.; Boehnke, N.; Deik, A. A.; Reinhardt, F.; Eaton, J. K.; Ferguson, B.; Wang, W.; Fairman, J.; Keys, H. R.; Danck, V.; Clish, C. B.; Clemons, P. A.; Hammond, P. T.; Boyer, L. A.; Weinberg, R. A.; Schreiber, S. L. Plasticity of Ether Lipids Promotes Ferroptosis Susceptibility and Evasion. *Nature* **2020**, *585*, 603−608. (m) Martin, B.; Vigneron, J. P.; Oudrhiri, N.; Fauquet, M.; Vergely, L.; Bradley, J. C.; Basseville, M.; Lehn, P.; Lehn, J. M. Guanidinium-Cholesterol Cationic Lipids: Efficient Vectors for the Transfection of Eukaryotic Cells. *Proc. Natl. Acad. Sci. U. S. A.* **1996**, *93*, 9682−9686. (n) Sainlos, M.; Aissaoui, A.; Oudrhiri, N.; Hauchecorne, M.; Vigneron, J. P.; Lehn, J. M.; Lehn, P. The Design of Cationic Lipids for Gene Delivery. *Curr. Pharm. Des.* **2005**, *11*, 375−394. (o) Haluska, C. K.; Riske, K. A.; Marchi-Artzner, V.; Lehn, J.-M.; Lipowsky, R.; Dimova, R. Time Scales of Membrane Fusion Revealed by Direct Imaging of Vesicle Fusion with High Temporal Resolution. *Proc. Natl. Acad. Sci. U. S. A.* **2006**, *103*, 15841−15846. (p) Kohata, A.; Hashim, P. K.; Okuro, K.; Aida, T. Transferrin Appended Nanocaplet for Transcellular siRNA Delivery into Deep Tissues. *J. Am. Chem. Soc.* **2019**, *141*, 2862−2866.

(11) (a) Discher, B. M.; Won, Y.-Y.; Ege, D. S.; Lee, J. C. M.; Bates, F. S.; Discher, D. E.; Hammer, D. A. Polymersomes: Tough Vesicles Made from Diblock Copolymers. *Science* **1999**, *284*, 1143−1146. (b) Discher, D. E.; Ortiz, V.; Srinivas, G.; Klein, M. L.; Kim, Y.; Christian, D.; Cai, S.; Photos, P.; Ahmed, F. Emerging Applications of Polymersomes in Delivery: From Molecular Dynamics to Shrinkage of Tumors. *Prog. Polym. Sci.* **2007**, *32*, 838−857. (c) Bellomo, E. G.; Wyrsta, M. D.; Pakstis, L.; Pochan, D. J.; Deming, T. J. Stimuli-Responsive Polypeptide Vesicles by Conformation-Specific Assembly. *Nat. Mater.* **2004**, *3*, 244−248. (d) Elsabahy, M.; Heo, G. S.; Lim, S. M.; Sun, G.; Wooley, K. L. Polymeric Nanostructures for Imaging and Therapy. *Chem. Rev.* **2015**, *115*, 10967−11011.

https://doi.org/10.1021/jacs.1c05813
J. Am. Chem. Soc. XXXX, XXX, XXX−XXX

(12) (a) Percec, V.; Wilson, D. A.; Leowanawat, P.; Wilson, C. J.; Hughes, A. D.; Kaucher, M. S.; Hammer, D. A.; Levine, D. H.; Kim, A. J.; Bates, F. S.; Davis, K. P.; Lodge, T. P.; Klein, M. L.; DeVane, R. H.; Aqad, E.; Rosen, B. M.; Argintaru, A. O.; Sienkowska, M. J.; Rissanen, K.; Nummelin, S. Self-Assembly of Janus Dendrimers into Uniform Dendrimersomes and Other Complex Architectures. *Science* **2010**, *328*, 1009−1014. (b) Sherman, S. E.; Xiao, Q.; Percec, V. Mimicking Complex Biological Membranes and Their Programmable Glycan Ligands with Dendrimersomes and Glycodendrimersomes. *Chem. Rev.* **2017**, *117*, 6538−6631. (c) Peterca, M.; Percec, V.; Leowanawat, P.; Bertin, A. Predicting the Size and Properties of Dendrimersomes from the Lamellar Structure of Their Amphiphilic Janus Dendrimers. *J. Am. Chem. Soc.* **2011**, *133*, 20507−20520. (d) Zhang, S.; Sun, H.-J.; Hughes, A. D.; Draghici, B.; Lejnieks, J.; Leowanawat, P.; Bertin, A.; Otero De Leon, L.; Kulikov, O. V.; Chen, Y.; Pochan, D. J.; Heiney, P. A.; Percec, V. Single-Single" Amphiphilic Janus Dendrimers Self-Assemble into Uniform Dendrimersomes with Predictable Size. *ACS Nano* **2014**, *8*, 1554−1565. (e) Zhang, S.; Sun, H.-J.; Hughes, A. D.; Moussodia, R.-O.; Bertin, A.; Chen, Y.; Pochan, D. J.; Heiney, P. A.; Klein, M. L.; Percec, V. Self-Assembly of Amphiphilic Janus Dendrimers into Uniform Onion-Like Dendrimersomes with Predictable Size and Number of Bilayers. *Proc. Natl. Acad. Sci. U. S. A.* **2014**, *111*, 9058−9063. (f) Xiao, Q.; Yadavalli, S. S.; Zhang, S.; Sherman, S. E.; Fiorin, E.; Silva, L. d.; Wilson, D. A.; Hammer, D. A.; André, S.; Gabius, H.-J.; Klein, M. L.; Goulian, M.; Percec, V. Bioactive Cell-Like Hybrids Coassembled from (Glyco)-Dendrimersomes with Bacterial Membranes. *Proc. Natl. Acad. Sci. U. S. A.* **2016**, *113*, E1134−E1141. (g) Yadavalli, S. S.; Xiao, Q.; Sherman, S. E.; Hasley, W. D.; Klein, M. L.; Goulian, M.; Percec, V. Bioactive Cell-Like Hybrids from Dendrimersomes with a Human Cell Membrane and Its Components. *Proc. Natl. Acad. Sci. U. S. A.* **2019**, *116*, 744−752. (h) Xiao, Q.; Sherman, S. E.; Wilner, S. E.; Zhou, X.; Dazen, C.; Baumgart, T.; Reed, E. H.; Hammer, D. A.; Shinoda, W.; Klein, M. L.; Percec, V. Janus Dendrimersomes Coassembled from Fluorinated, Hydrogenated, and Hybrid Janus Dendrimers as Models for Cell Fusion and Fission. *Proc. Natl. Acad. Sci. U. S. A.* **2017**, *114*, E7045−E7053. (i) Torre, P.; Xiao, Q.; Buzzacchera, I.; Sherman, S. E.; Rahimi, K.; Kostina, N. Y.; Rodriguez-Emmenegger, C.; Möller, M.; Wilson, C. J.; Klein, M. L.; Good, M. C.; Percec, V. Encapsulation of Hydrophobic Components in Dendrimersomes and Decoration of Their Surface with Proteins and Nucleic Acids. *Proc. Natl. Acad. Sci. U. S. A.* **2019**, *116*, 15378−15385. (j) Li, S.; Xia, B.; Javed, B.; Hasley, W. D.; Melendez-Davila, A.; Liu, M.; Kerzner, M.; Agarwal, S.; Xiao, Q.; Torre, P.; Bermudez, J. G.; Rahimi, K.; Kostina, N. Yu.; Möller, M.; Rodriguez-Emmenegger, C.; Klein, M. L.; Percec, V.; Good, M. C. Direct Visualization of Vesicle Disassembly and Reassembly Using Photocleavable Dendrimers Elucidates Cargo Release Mechanisms. *ACS Nano* **2020**, *14*, 7398−7411. (k) Kostina, N. Y.; Wagner, A. M.; Haraszti, T.; Rahimi, K.; Xiao, Q.; Klein, M. L.; Percec, V.; Rodriguez-Emmenegger, C. Unraveling Topology-Induced Shape Transformations in Dendrimersomes. *Soft Matter* **2021**, *17*, 254−267. (l) Kostina, N. Yu.; Rahimi, K.; Xiao, Q.; Haraszti, T.; Dedisch, S.; Spatz, J. P.; Schwaneberg, U.; Klein, M. L.; Percec, V.; Möller, M.; Rodriguez-Emmenegger, C. Membrane-Mimetic Dendrimersomes Engulf Living Bacteria via Endocytosis. *Nano Lett.* **2019**, *19*, 5732−5738. (m) Buzzacchera, I.; Xiao, Q.; Han, H.; Rahimi, K.; Li, S.; Kostina, N. Y.; Toebes, B. J.; Wilner, S. E.; Möller, M.; Rodriguez-Emmenegger, C.; Baumgart, T.; Wilson, D. A.; Wilson, C. J.; Klein, M. L.; Percec, V. Screening Libraries of Amphiphilic Janus Dendrimers based on Natural Phenolic Acids to Discover Monodisperse Unilamellar Dendrimersomes. *Biomacromolecules* **2019**, *20*, 712−727.

(13) (a) Percec, V.; Leowanawat, P.; Sun, H.-J.; Kulikov, O.; Nusbaum, C. D.; Tran, T. M.; Bertin, A.; Wilson, D. A.; Peterca, M.; Zhang, S.; Kamat, N. P.; Vargo, K.; Moock, D.; Johnston, E. D.; Hammer, D. A.; Pochan, D. J.; Chen, Y.; Chabre, Y. M.; Shiao, T. C.; Bergeron-Brlek, M.; Andre, S.; Roy, R.; Gabius, H.-J.; Heiney, P. A. Modular Synthesis of Amphiphilic Janus Glycodendrimers and Their Self-Assembly into Glycodendrimersomes and Other Complex Architectures with Bioactivity to Biomedically Relevant Lectins. *J. Am. Chem. Soc.* **2013**, *135*, 9055−9077. (b) Zhang, S.; Xiao, Q.; Sherman, S. E.; Muncan, A.; Ramos Vicente, A. D. M.; Wang, Z.; Hammer, D. A.; Williams, D.; Chen, Y.; Pochan, D. J.; Vértesy, S.; André, S.; Klein, M. L.; Gabius, H.-J.; Percec, V. Glycodendrimersomes from Sequence-Defined Janus Glycodendrimers Reveal High Activity and Sensor Capacity for the Agglutination by Natural Variants of Human Lectins. *J. Am. Chem. Soc.* **2015**, *137*, 13334−13344. (c) Xiao, Q.; Zhang, S.; Wang, Z.; Sherman, S. E.; Moussodia, R.-O.; Peterca, M.; Muncan, A.; Williams, D. R.; Hammer, D. A.; Vértesy, S.; André, S.; Gabius, H.-J.; Klein, M. L.; Percec, V. Onion-like Glycodendrimersomes from Sequence-Defined Janus Glycodendrimers and Influence of Architecture on Reactivity to a Lectin. *Proc. Natl. Acad. Sci. U. S. A.* **2016**, *113*, 1162−1167. (d) Rodriguez-Emmenegger, C.; Xiao, Q.; Kostina, N. Y.; Sherman, S. E.; Rahimi, K.; Partridge, B. E.; Li, S.; Sahoo, D.; Perez, A. M. R.; Buzzacchera, I.; Han, H.; Kerzner, M.; Malhotra, I.; Möller, M.; Wilson, C. J.; Good, M. C.; Goulian, M.; Baumgart, T.; Klein, M. L.; Virgil Percec, V. Encoding Biological Recognition in a Bicomponent Cell-Membrane Mimic. *Proc. Natl. Acad. Sci. U. S. A.* **2019**, *116*, 5376−5382. (e) Xiao, Q.; Delbianco, M.; Sherman, S. E.; Perez, A. M. R.; Bharate, P.; Pardo-Vargas, A.; Rodriguez-Emmenegger, C.; Kostina, N. Y.; Rahimi, K.; Söder, D.; Möller, M.; Klein, M. L.; Seeberger, P. H.; Percec, V. Nanovesicles Displaying Functional Linear and Branched Oligomannose Self-Assembled from Sequence-Defined Janus Glycodendrimers. *Proc. Natl. Acad. Sci. U. S. A.* **2020**, *117*, 11931−11939. (f) Kostina, N. Y.; Söder, D.; Haraszti, T.; Xiao, Q.; Rahimi, K.; Partridge, B. E.; Klein, M. L.; Percec, V.; Rodriguez-Emmenegger, C. Enhanced Concanavalin A Binding to Preorganized Mannose Nanoarrays in Glycodendrimersomes Revealed Multivalent Interactions. *Angew. Chem., Int. Ed.* **2021**, *60*, 8352−8360.

(14) (a) Ramishetti, S.; Hazan-Halevy, I.; Palakuri, R.; Chatterjee, S.; Gonna, S. N.; Dammes, N.; Freilich, I.; Shmuel, L. K.; Danino, D.; Peer, D. A Combinatorial Library of Lipid Nanoparticles for RNA Delivery to Leukocytes. *Adv. Mater.* **2020**, *32*, 1906128. (b) Kim, M.; Jeong, M.; Hur, S.; Cho, Y.; Park, J.; Jung, H.; Seo, Y.; Woo, H. A.; Nam, K. T.; Lee, K.; Lee, H. Engineered Ionizable Lipid Nanoparticles for Targeted Delivery of RNA Therapeutics into Different Types of Cells in the Liver. *Sci. Adv.* **2021**, *7*, No. eabf4398.

(15) Huotari, J.; Helenius, A. Endosome Maturation. *EMBO J.* **2011**, *30*, 3481−3500.

(16) Horita, K.; Yoshioka, T.; Tanaka, T.; Oikawa, Y.; Yonemitsu, O. On the Selectivity of Deprotection of Benzyl, MPM (4-Methoxybenzyl) and DMPM (3,4-Dimethoxybenzyl) Protecting Groups for Hydroxy Functions. *Tetrahedron* **1986**, *42*, 3021−3028.

(17) (a) Levitt, M.; Perutz, M. F. Aromatic Rings Act as Hydrogen Bond Acceptors. *J. Mol. Biol.* **1988**, *201*, 751−754. (b) Perutz, M. F.; Kirby, A. J.; Williams, D. H. The Role of Aromatic Rings as Hydrogen-Bond Acceptors in Molecular Recognition. *Philos. Trans. R. Soc., A* **1993**, *345*, 105−112. (c) Perutz, M. F.; Fermi, G.; Abraham, D. J.; Poyart, C.; Bursaux, E. Hemoglobin as a Receptor of Drugs and Peptides: X-Ray Studies of the Stereochemistry of Binding. *J. Am. Chem. Soc.* **1986**, *108*, 1064−1078. (d) Loewenthal, R.; Sancho, J.; Fersht, A. R. Histidine-Aromatic Interactions in Barnase: Elevation of Histidine PKa and Contribution to Protein Stability. *J. Mol. Biol.* **1992**, *224*, 759−770. (e) Zacharias, N.; Dougherty, D. A. Cation-π Interactions in Ligand Recognition and Catalysis. *Trends Pharmacol. Sci.* **2002**, *23*, 281−287. (f) Gallivan, J. P.; Dougherty, D. A. Cation-π Interactions in Structural Biology. *Proc. Natl. Acad. Sci. U. S. A.* **1999**, *96*, 9459−9464. (g) Dougherty, D. A. Cation-π Interactions in Chemistry and Biology: A New View of Benzene, Phe, Tyr, and Trp. *Science* **1996**, *271*, 163−168. (h) Dougherty, D. A. The Cation-π Interaction. *Acc. Chem. Res.* **2013**, *46*, 885−893. (i) Ma, J. C.; Dougherty, D. A. The Cation-π Interaction. *Chem. Rev.* **1997**, *97*, 1303−1324. (j) Dougherty, D. A.; Stauffer, D. A. Acetylcholine Binding by a Synthetic Receptor: Implications for Biological Recognition. *Science* **1990**, *250*, 1558−1560.

(18) (a) Karikó, K.; Buckstein, M.; Ni, H.; Weissman, D. Suppression of RNA Recognition by Toll-like Receptors: The Impact

https://doi.org/10.1021/jacs.1c05813
J. Am. Chem. Soc. XXXX, XXX, XXX−XXX

of Nucleoside Modification and the Evolutionary Origin of RNA. *Immunity* **2005**, *23*, 165−175. (b) Pardi, N.; Muramatsu, H.; Weissman, D.; Kariko, K. In Vitro Transcription of Long RNA Containing Modified Nucleosides. *Methods Mol. Biol.* **2013**, *969*, 29−42.

(19) (a) Khan, O. F.; Zaia, E. W.; Jhunjhunwala, S.; Xue, W.; Cai, W. X.; Yun, D. S.; Barnes, C. M.; Dahlman, J. E.; Dong, Y. Z.; Pelet, J. M.; Webber, M. J.; Tsosie, J. K.; Jacks, T. E.; Langer, R.; Anderson, D. G. Dendrimer-Inspired Nanomaterials for the in Vivo Delivery of siRNA to Lung Vasculature. *Nano Lett.* **2015**, *15*, 3008−3016. (b) Patel, A. K.; Kaczmarek, J. C.; Bose, S.; Kauffman, K. J.; Mir, F.; Heartlein, M. W.; DeRosa, F.; Langer, R.; Anderson, D. G. Inhaled Nanoformulated mRNA Polyplexes for Protein Production in Lung Epithelium. *Adv. Mater.* **2019**, *31*, 1805116.

(20) (a) Lehn, J. M. Toward Self-Organization and Complex Matter. *Science* **2002**, *295*, 2400−2403. (b) Rosen, B. M.; Wilson, C. J.; Wilson, D. A.; Peterca, M.; Imam, M. R.; Percec, V. Dendron-Mediated Self-Assembly, Disassembly, and Self-Organization of Complex Systems. *Chem. Rev.* **2009**, *109*, 6275−6540.

https://doi.org/10.1021/jacs.1c05813
J. Am. Chem. Soc. XXXX, XXX, XXX−XXX